# A CFD ANALYSIS OF LIQUID HYDROGEN VESSEL EXPLOSIONS USING THE ADREA-HF CODE

**Ustolin, F.[1,2*], Tolias, I.C.[2], Giannissi, S.G.[2], Venetsanos, A.G.[2] and Paltrinieri, N.[1]**
**[1] Department of Mechanical and Industrial Engineering, Norwegian University of Science and Technology NTNU, S.P. Andersens veg 3, Trondheim, 7031, Norway, *federico.ustolin@ntnu.no**
**[2] Environmental Research Laboratory, National Centre for Scientific Research "Demokritos", Aghia Paraskevi, Attikis, 15341, Greece**

**ABSTRACT**

Despite hydrogen is one of the most suitable candidates in replacing fossil fuels, its very low density represents a drawback when it is stored. The liquefaction process can increase the hydrogen density and therefore enhance its storage capacity. The boiling liquid expanding vapour explosion (BLEVE) is a typical accident scenario that must be always considered when liquefied gases are stored. In particular, BLEVE is a physical explosion with low probabilities and high consequences which may occur after the catastrophic rupture of a vessel containing a liquid with a temperature above its boiling point at atmospheric pressure. In this paper, a parametric CFD analysis of the BLEVE phenomenon was conducted by means of the CFD code ADREA-HF for liquid hydrogen ($LH_2$) vessels. Firstly, the CFD model is validated against a well-documented $CO_2$ BLEVE experiment. Next, hydrogen BLEVE cases are examined. The physical parameters were chosen based on the BMW tests carried out in the 1990s on $LH_2$ tanks designed for automotive purposes. Different filling degrees, initial pressures and temperatures of the tank content are simulated to comprehend how the blast wave is influenced by the initial conditions. The aim of this study is twofold: provide new insights and observations on the BLEVE dynamics and demonstrate the CFD tool effectiveness for conducting the consequence analysis and thus aiding the risk assessment of liquefied gas vessel explosion. Good agreement was shown between the simulation outcomes and the experimental results.

## 1.0 INTRODUCTION

The employment of low or zero emissions fuels must increase in the near future to fight the global warming and reduce the environmental pollution. Hydrogen is potentially clean and renewable depending how it is utilised and produced [1]. Furthermore, it can be employed as energy carrier and solve the intermittency issue related to renewable energies such as solar and wind. Despite hydrogen has a high gravimetric energy density (119.96 MJ $kg^{-1}$ [2]), its density is extremely low (0.0852 kg $m^{-3}$ at 15°C and atmospheric pressure [3]). The liquefaction process is one of the most suitable method to increase the hydrogen density. Liquid hydrogen ($LH_2$) is a cryogenic fluid at atmospheric pressure since its boiling point is extremely low (20.3 K at atmospheric pressure [3]). It is usually stored in tanks composed by an inner and outer shells separated by vacuum jacket filled with different type of insulation (mainly perlite or multi-layer insulation, MLI) [4]. Since the global hydrogen consumption is expected to grow from now to 2050 as aftermath of the COVID-19 pandemic [5], large amounts of this fuel can be stored in liquid form. For instance, different $LH_2$ fuelled ships are planned to be in operation within few years, such as the MF Hydra, the world's first $LH_2$ powered ferry [6], or the Topeka vessel, result of the HySHIP project [7]. Hydrogen can be categorised based on its production process as grey, blue, or green [8]. Green hydrogen is produced from water through electrolysis by exploiting the electric energy generated from renewable sources. This is the cleanest method to produce hydrogen (potentially carbon neutral) as well as the most expensive due to the costs of renewable electricity and electrolysers [8]. However, it is foreseen that these costs will be decreased in the European area in the next decades [9]. Grey hydrogen is extracted from hydrocarbons (e.g. natural gas) mainly through steam reforming which is currently one of the cheapest techniques. This method is also the most pollutant hydrogen production process since large amounts of $CO_2$ are released in the atmosphere. If the carbon capture and storage (CCS) is applied to the steam reforming process, the greenhouse gas (GHG) footprint can be considerably reduced. In this manner, blue hydrogen is obtained. Moreover, it seems that a good compromise between costs and low emission is met by the blue hydrogen production. For this reason, this technique will be exploited in the next decade as transition from grey to green hydrogen. Therefore, it is highly likely that both hydrogen and $CO_2$ storage systems will be present in the same production facility, and the safety aspects related to these substances must be evaluated.

Among different critical events, the catastrophic rupture of the tank must be always considered during the risk assessment of liquefied gas vessels [10]. One of the consequences of this critical event is the boiling liquid expanding vapour explosion (BLEVE). This is a physical explosion generated by the expansion of the compressed vapour phase and the flashing of the superheated liquid. Its consequences are the pressure wave, the fragments thrown away by the explosion and the fireball if the substance is flammable. Occasionally BLEVE is not considered as direct consequence of the catastrophic rupture of the tank yet as a domino effect due to its very low probability to happen [11]. In the past, several BLEVE accidents occurred for different type of substances including $CO_2$ and $LH_2$ [12], and continue to happen as for the propane tank truck accident in Bologna, Italy, in August 2018 [13]. Furthermore, hydrogen should be considered as an emerging technology when applied in new applications such as the maritime field [14]. For these reasons and because BLEVE has severe consequences, this explosion must be always considered during the risk assessment of liquefied gas vessels. In 1957, the term BLEVE was coined for the first time by Walls [15,16]. Despite, numerous research studies were conducted on this phenomenon since then, an unequivocal theory to properly explain this type of explosion does not exist. This can be demonstrated by the development of different analytical models to estimate the mechanical energy generated by the explosion and thus determine the overpressure and impulse of the blast wave [17,18]. Even different BLEVE definitions were proposed in the literature [12,19]. The complexity of the phenomenon and the lack of experiments for different substances, such as $LH_2$, may be the origins of these disagreements.

In this study, the pressure waves generated by the BLEVE explosion of a $CO_2$ bottle and a $LH_2$ tank were numerically simulated and investigated by means of the ADREA-HF CFD code. The aim was to provide critical indications on the BLEVE theory. The state-of-the-art of the BLEVE CFD analysis for different substances is presented. Therefore, the CFD code was validated by comparing the results of a liquid CO2 ($LCO_2$) explosion test with the numerical simulation outcomes. The same approach was adopted to conduct a CFD parametric analysis of a $LH_2$ tank by changing the initial conditions i.e., pressure, temperature and hydrogen mass. In particular, the BMW bursting scenario tests published in [20] were replicated during this analysis. Therefore, the CFD analysis of a BLEVE explosion of cryogenic fluid ($LH_2$) as well as the CFD simulation of the BMW tests were conducted for the first time. Good agreement was shown when the CFD outcomes were compared with the experimental results. However, additional experiments are required to further validate the CFD code, especially in the case of $LH_2$. For this reason, during the "Safe Hydrogen Fuel Handling and Use for Efficient Implementation ($SH_2IFT$)" project, fire tests will be conducted on three different double walled $LH_2$ tanks with the goal of achieving a BLEVE [21]. Moreover, $LH_2$ BLEVE phenomenon has been investigated as well during the "Prenormative Research for Safe Use of Liquid Hydrogen" (PRESLHY) [22]

## 2.0 BLEVE TESTS

In this section, the explosion tests considered in this study are described. Firstly, the details of the $CO_2$ experiments conducted by Van der Voort et al. [23] and employed in this paper to validate the CFD code are provided. Secondly, the explosion tests on the $LH_2$ tank conducted during the 1990's by BMW car manufacturer [20] are presented.

### 2.1 $LCO_2$ BLEVE

In 2012, Van der Voort et al. [23] conducted an explosion test on a 40-l bottle of $CO_2$ at the Laboratory for Ballistic Research (TNO Defence, Security and Safety) in a test bunker with the following dimensions: 6 × 12 × 4 m. The cylindrical steel bottle with a diameter of 0.23 m and height of 1.37 m was placed vertically on the floor at the centre of the bunker and filled for more than 95% with superheated $LCO_2$ at a temperature of 290 K and pressure of approx. 5.2 MPa [23]. The bottle was wrecked by two linear-shaped explosive charges with 1 m length attached at two opposite sides of the cylinder in the axial direction. The results of this type of experiment can be used to analyse the BLEVE pressure wave and for validation purposes since the rupture of the vessel was rapid and complete, there was not chemical reaction (combustion), and the bottle was virtually full of liquid. However, the reflections of the blast wave on the bunker walls generated disturbances in the overpressure measurements. The authors suggested to replicate the experiments in a free field test site and measure the pressure wave along different axes to investigate its directionality provoked by the chaotic fracture of the container [23].

### 3.2 BMW safety tests for $LH_2$ tanks

In 1979, BMW car manufacturer presented the first hydrogen-fuelled vehicle powered by an internal combustion engine [24]. In 2005, BMW produced the first customer car with an $LH_2$ storage system installed onboard: the BMW Hydrogen 7. This car could be fuelled by either diesel or hydrogen fuels. In this case, hydrogen was stored in cryogenic liquid form inside a double walled tank which was composed by two vessels (inner and outer tanks) separated by a vacuum jacket. The multi-layer insulation (MLI) was wrapped around the inner container in order to limit the heat losses, and thus the evaporation of the tank content. The vessel was developed by BMW in collaboration mainly with Messer Griesheim GmbH, Linde AG [20]. Several safety requirements had to be met in order to certify and commercialise this hydrogen car with and its $LH_2$ storage system. For this reason, a safety research program on the $LH_2$ car was initiated in 1992. Various tests were conducted by BMW either on the entire vehicle (e.g. crash test) [24] or on the $LH_2$ storage system (e.g. vacuum loss, fire and burst tests) [25]. The bursting tank scenario was investigated and presented by Pehr in [20]. During this test series, a total of ten tanks containing different amounts of $LH_2$ (1.8 ÷ 5.4 kg) were destroyed at different pressures (2 ÷ 14.8 bar). Only the inner tanks, with an internal volume of 0.12 $m^3$, were tested and the rupture was initiated by explosives. The description of this experiments recalls a cold BLEVE explosion since the tank was not engulfed in a fire. However, fireballs were generated due to the presence of ignition source (cutting charges). Although this investigation is quite unique and provides critical information on the explosion of medium-scale $LH_2$ tanks, several uncertainties were present during the test and encumber the analysis of the results. For instance, the exact $LH_2$ mass could not be measured during each test because the level sensor was working imprecisely at high pressures [20]. Moreover, only the maximum value of overpressure was reported, and this value was the average of three different measuring points placed at 3 m from the tank centre. Hence, the directionality of the blast wave and its impulse cannot be analysed. During test 3 and 7, over-proportional overpressure results were measured and do not seem to be reliable outcomes. Only the maximum fireball diameter (20 m) and duration (4 s) were documented in the paper as well as the maximum horizontal distance reached by the fragments thrown away by the explosion (> 15 m) [20]. For all these reasons, a proper validation cannot be performed by exploiting these results. Nevertheless, they may be used as reference for comparison purposes with the outcomes of the numerical simulations.

## 3.0 CFD ANALYSIS BY USING THE ADREA-HF CODE

The ADREA-HF CFD code was selected to numerically simulate the BLEVE of $LCO_2$ and $LH_2$ vessels. ADREA-HF code [26] is 3D time dependent finite volume code, which is validated against several experiments involving flammable gas dispersion [27–30] and combustion [31–33]. It solves the conservation equations of mass, momentum and energy for the mixture along with the species total mass fraction conservation equation. ADREA-HF code has several turbulence modelling approaches available, RANS type and LES. It can handle multi-phase multi-component mixtures using the Eulerian methodology and assuming that the non-vapor (liquid and/or solid phase) is dispersed in the vapor mixture. By default, the Homogeneous Equilibrium Model (HEM) is used, i.e. the phases have the same velocity and share the same temperature. However, there is also the option of Non-Homogeneous Equilibrium Model (NHEM), in which the phases (vapor and non-vapor) can develop different velocities [32]. For the phase distribution of components, the Raoult's law for ideal mixture is used and the Rachford-Rice (R-C) methodology is employed, which is effective for multi-component mixtures [32]. In this study, the code was validated with the $LCO_2$ BLEVE experiments described in Sec. 2.1. Afterward, a parametric analysis of the explosion of the $LH_2$ vessel was performed with the validated CFD code and a similar approach. The $LH_2$ vessel burst test series presented in Sec. 2.2 were replicated and the simulation outcomes were compared with the experimental results.

### 3.1 Governing equations

The Navier-Stokes equations, the continuity equation and the energy equation of the mixture are solved along with the conservation equation of species. The Favre-averaged equations are (Einstein summation convention is used):

$$\frac{\partial \bar{\rho}}{\partial t} + \frac{\partial \bar{\rho}\tilde{u}_i}{\partial x_i} = 0, \tag{1}$$

$$\frac{\partial \bar{\rho}\tilde{u}_i}{\partial t} + \frac{\partial \bar{\rho}\tilde{u}_j\tilde{u}_i}{\partial x_j} = -\frac{\partial \bar{p}}{\partial x_i} + \frac{\partial}{\partial x_j}\left(\mu_{eff}\left(\frac{\partial \tilde{u}_i}{\partial x_j} + \frac{\partial \tilde{u}_j}{\partial x_i}\right)\right) + \bar{\rho}g_i, \tag{2}$$

$$\frac{\partial \bar{\rho}\tilde{H}}{\partial t} + \frac{\partial \bar{\rho}\tilde{u}_j\tilde{H}}{\partial x_j} = \frac{\partial}{\partial x_j}\left(\frac{\mu_t}{Pr_t}\frac{\partial \tilde{H}}{\partial x_j}\right) + \frac{D\bar{p}}{Dt}, \tag{3}$$

$$\frac{\partial \bar{\rho}\tilde{q}_k}{\partial t} + \frac{\partial \bar{\rho}\tilde{u}_j\tilde{q}_k}{\partial x_j} = \frac{\partial}{\partial x_j}\left(\frac{\mu_t}{Sc_t}\frac{\partial \tilde{q}_k}{\partial x_j}\right) + \bar{R}_k, \quad k = 1, \ldots, N_{subs}, \tag{4}$$

Turbulence is modelled using the standard k-ε model with wall functions. The temperature of the mixture and the phase distribution of the species are calculated using the Raoult's law for ideal mixtures, given the pressure, the mixture enthalpy and the species mass fractions. Non-vapor phase exists only if the temperature of the mixture is lower than its dew temperature. In that case, if the temperature is higher than the triple point, liquid phase is considered otherwise solid phase. ADREA-HF code contains an extensive thermodynamic package with physical properties of many elements and compounds. A number of different equations of state are also included. The simplest model makes a discrete description of each phase (ideal gas, correlations for the density of liquid and solid phase as a function of temperature). Third order equations of state are also available such as Peng Robinson and Redlich-Kwong-Mathias-Copeman (RKMC). For the current work, both Peng Robinson and RKMC EoS were tested. RKMC was chosen since it seems to be the most accurate and robust EoS for estimating the hydrogen properties at saturated and supercritical conditions [33]. The differences in the results were negligible.

### 3.2 Numerical details

ADREA-HF uses the finite volume method on a staggered Cartesian grid. The pressure and velocity equations are decoupled using a modification of the SIMPLER algorithm. For the discretization of the convective terms a second order accurate bounded scheme was used. For the time advancement, first order backward differences were chosen. The time step is automatically adapted according to prescribed error bands and the desired CFL number. Very small time-steps were used in order to ensure numerical stability and convergence. CFL maximum value was equal to 0.01 in all cases.

### 3.3 Configuration of the $LCO_2$ explosion simulations

For the $LCO_2$ simulations a rectangular region of 40-liters volume $LCO_2$ was placed at the centre of the domain with dimensions equal to the experimental room dimensions (6 × 12 × 4 m). The rectangular region modelled in close approximation the $CO_2$ cylinder with height around 1.1 m and base area 0.036 $m^2$. It was assumed that the bottle rupture was instantaneous and uniform in all the directions, therefore the vessel content was subjected to a sudden depressurisation. Since during the experiments the bottle was filled for more than 95% [23], only liquid $CO_2$ at saturation conditions was considered within the tank region in the CFD analysis. Finally, the effect of the cutting charges, installed along the vertical axis of the bottle to break it, was not considered. Table 1 shows the initial condition for the simulation.

Table 1. Initial conditions of the $LCO_2$ BLEVE simulation.

| Pressure (Pa) | Temperature (K) | Density ($kg/m^3$) | Mass (kg) |
|---|---|---|---|
| 5,200,000 | 289.03 | 772.54 | 30.90 |

The computational domain was limited by the room walls and double symmetry along y- and x-axis was assumed. Four different grid sizes were tested with 33,792 (grid1), 113,960 (grid2), 265,832 (grid3), 469,560 (grid4) cells to achieve grid independence. The results of the grid independency study are shown in Fig. 1. The relative error between grid 3 and 4 is lower than or around 1% for all three sensors, thus grid3 provides independent results. The simulation with grid3 is compared with the experimental results in Sec. 4.1. Wall boundary conditions (BC) were set at all boundaries except for the symmetry planes, where symmetry BC were imposed.

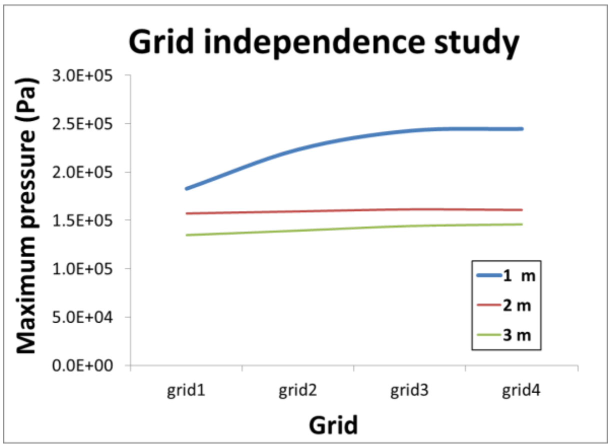


Figure 1. Grid independency study for LCO2 simulations.

### 3.2 Configuration of the $LH_2$ explosion simulations

In the $LH_2$ BLEVE CFD parametric analysis, the tank used in the BMW tests was simulated. The 120-liters cylindrical vessel was approximated by a prismatic tank with a height of 0.706 m and 0.177 $m^2$ base. The container was placed horizontally in the domain, at 1 m from the ground, and the double symmetry along the transversal and longitudinal tank axes (x and y directions) was exploited. Therefore, only ¼ of the tank was included in the domain which had a size of 10 × 10 × 11 m along the x, y, z axes. In Table 2, a summary of the simulated $LH_2$ and $LCO_2$ tanks characteristics and dimensions of the domains is presented for comparison purpose.

Table 2. Characteristics of the simulated $LH_2$ and $LCO_2$ tanks and dimensions of the domains.

| Tank | Volume (litres) | Area ($m^2$) | Height (m) | Orientation | Height from the ground (m) | Domain dimensions (m) |
|---|---|---|---|---|---|---|
| $LCO_2$ | 40 | 0.036 | 1.100 | Vertical | 0 | 3 × 6 × 4 |
| $LH_2$ | 120 | 0.177 | 0.706 | Horizontal | 1 | 10 × 10 × 11 |

A grid sensitivity analysis was conducted, thus the minimum cell size to achieve grid independence was ca. 0.029 m in all directions. Therefore, the quarter of the tank was composed by 1,176 cells. The mesh was kept uniform around the vessel and then stretched with a growing factor of 1.1. The total number of cells in the domain was 1,268,592. Inside the tank region, the hydrogen was assumed to be in both liquid and vapour phase at saturation conditions at the given pressure. Only one pressure level was investigated: the 11 bar case. The $LH_2$ mass was varied in each simulation. In addition, it was possible to analyse the dynamic of the blast wave and how it is affected by the two phases by simulating the tank full of either liquid or gaseous hydrogen. In this latter case, the simulated explosion is not a BLEVE but it was exploited as comparison. In Table 3, the different configurations selected for the parametric analysis are collected. Several parameters such pressure, temperature and density were recorded at different points. The sensors were placed inside the vessel, in the proximity of the tank wall (at 0.1 m) and at 3.0 m from the tank centre along all the three axes (x, y and z) in order to analyse the pressure wave generated by the explosion. The horizontal plane (x-y) which intercepts the tank transversal and longitudinal axes was at 1.2 m from the ground, at the same height of the vessel centre line.

Table 3. Initial conditions of the $LH_2$ BLEVE parametric analysis (abbreviations: L: liquid, V: vapour).

| Simulation | Phase and status | Pressure (Pa) | Temperature (K) | Density (kg/m$^3$) | Mass (kg) |
|---|---|---|---|---|---|
| LH2 | Saturated L | 1,101,325 | 32.10 | 42.42 | 1.27 |
| GH2 | Superheated V | | 32.93 | 15.00 | 0.45 |
| LH2-GH2 | L and V | | 32.10, 32.50 | 42.42, 16.30 | 0.77 |

A complete and instantaneous rupture of the vessel, hence a sudden depressurisation of the tank content was conservatively simulated. Finally, this analysis attempted to reproduce the BMW tests, in fact many analogies such as the tank volume, pressure level and $LH_2$ content can be noticed. However, few aspects were not taken into consideration in this study. For instance, the combustion of the hydrogen with a consequent fireball generation was not investigated, and the effect of the explosives employed to rupture the tank was neglected. For these reasons and due to the experimental uncertainties listed in Sec. 2.2, the CFD code could not be validated for $LH_2$ BLEVE.

## 4.0 RESULTS AND DISCUSSIONS

In this section, the results of the $LCO_2$ BLEVE CFD analysis conducted with the ADREA-HF code are reported. Afterwards, the outcomes of the parametric CFD analysis of the $LH_2$ BLEVE are analysed.

### 4.1 $LCO_2$ BLEVE CFD analysis and comparison with the experiments

Fig. 2 shows the overpressure time series for the experiment, the ADREA-HF simulation and the simulation of van der Voort et al. (with cylindrical symmetry) [23]. In the experiment, two peaks in overpressure can be observed. The initial peak is the blast wave caused by the cutting charges. Thus, only the second peak is compared with the simulations. According to Fig. 2, the blast wave is overpredicted for both models with ADREA-Hf simulation to have greater over prediction compared to van der Voort et al. [23] model at the closest sensors (at 1 m from the room centre) and lower at the rest sensors. Similarly, the negative overpressures are overestimated by both simulations. The ADREA-HF predicted peak overpressure is almost doubled the experimental one for the sensor B1, while for B2 the prediction has a relative error around 6%. The duration of the overpressure is almost the same for the simulations and slightly shorter than the experimental one, while the negative phase in B1and B2 is reproduced relatively well.

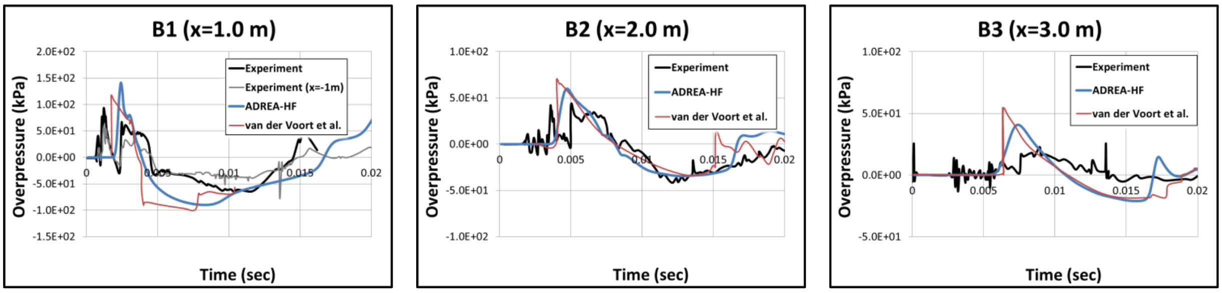


(a) (b) (c)

Figure 2. Pressure wave from the rupture of the $LCO_2$ bottle at (a) 1 m, (b) 2 m and (c) 3 m.

Furthermore, with the van der Voort et al. model the pressure increase is sharper, while with ADREA-HF code the increase is more smoothed. This can be attributed to the fact that van der Voort solves the Euler equations without molecular and turbulent diffusion terms. Apart from the overpressure, another significant parameter in BLEVE is the impulse. Table 4 summarizes the peak overpressure and the impulse for the experiment and the ADREA-HF simulation at sensors, B1, B2 and B3. The peak overpressure is overpredicted by a factor of around 1.5-2, as already observed in Fig. 2. Similarly, the impulse is overpredicted by a factor of 1.5-2, however this overprediction can be mainly attributed to the overpressure overestimation rather than the time duration of the overpressure, which is in satisfactory agreement with the experiment. Taking into account the experimental uncertainties and the agreement of the two computational codes, it can be concluded that ADREA-HF is capable of predicting the consequences of a BLEVE and can be used for the following $LH_2$ explosion analysis.

Table 4. Results of the $LCO_2$ BLEVE simulations: peak overpressure and impulse of the blast wave in three different positions.

| | Peak overpressure (kPa) | | | Impulse (kPa·s) | | |
|---|---|---|---|---|---|---|
| | B1 | B2 | B3 | B1 | B2 | B3 |
| Experiments | 67.00 | 43.93 | 25.64 | 0.1270 | 0.0834 | 0.0760 |
| ADREA-HF | 141.00 | 60.00 | 42.80 | 0.2500 | 0.1690 | 0.1130 |

### 4.2 $LH_2$ explosion simulations

In this section, the results achieved during the CFD parametric analysis of the $LH_2$ BLEVE are presented.

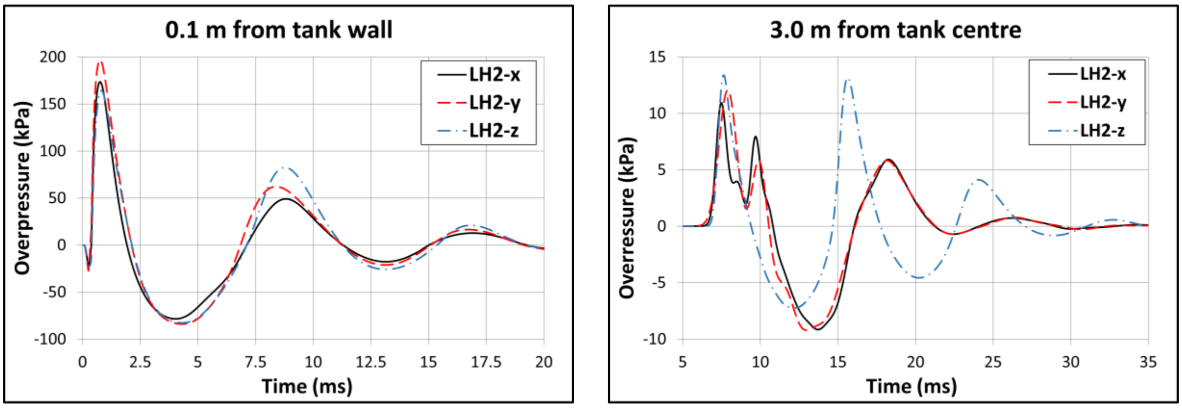


(a) (b)

Figure 3. Pressure wave generated by the depressurisation of the $LH_2$ tank with initial pressure of 11 bar at (a) 0.1 m from the tank wall and (b) 3.0 m from the tank centre along the three axes.

The overpressure variations in time along the three axes at different distances (0.1 m from the tank wall and 3.0 m from the tank centre) as outcome of the first configuration of Table 3 (100% liquid, 11 bar, 32.10 K) are reported in Fig. 3. Even though the overpressure is slightly higher in the y direction, the positive and negative phases as well as the reflection on the ground are developed at the same time. Instead, the pressure wave expands without any impediment in the vertical direction. Moreover, the intensity of the second pressure peak above the container is as high as the first peak. In addition, a third pressure peak is generated, as noticed in different BLEVE experimental tests [34,35], while it is almost imperceptible onward the horizontal axes. It was demonstrated that the liquid phase considerably influences the yield and the formation of both the second and third pressure peaks along all the directions. This phenomenon can be theoretically explained by the relatively slow phase change process of the liquid compared with the sudden expansion of the compressed gaseous phase [32]. The amount of $LH_2$ was reduced down to 0.47 kg (equivalent to a tank filling degree of 37%) in the LH2-GH2 simulation and replaced with gaseous hydrogen ($GH_2$) in the GH2 case. The comparison between these simulations is presented in Fig. 4, where the pressure was estimated again at 3.0 m from the tank centre. The first simulation (LH2) is kept in the charts as reference, and the y axis is not presented because these results are very similar to the x direction.

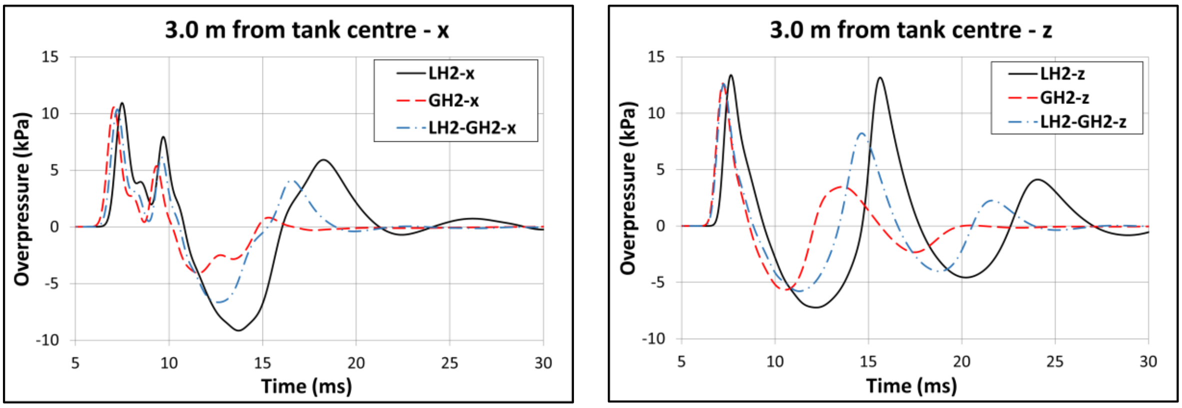


(a) (b)

Figure 4. Comparison of three different simulations with an initial tank pressure of 11 bar, in which the pressure was estimated at 3.0 m from the tank centre along the (a) x and (b) z axes.

It must be noticed that the third pressure peak was not generated during the LH2-GH2 and GH2 simulations along the horizontal axes, but only on the vertical direction if $LH_2$ was initially present in the tank. Furthermore, the explosion lasted more than 30 ms when the vessel was completely filled with $LH_2$, while the blast wave duration was reduced to approx. 25 and 20 ms when the filling degree was equal to 36% or barely $GH_2$ was initially present in the tank, respectively. An overview of the outcomes of the CFD parametric analysis of $LH_2$ BLEVE is provided in Table 5. In particular, the average of the maximum pressure wave overpressure and impulse values along the longitudinal, transversal and vertical axes at 3.0 m from the tank centre are collected. To summarise, the maximum overpressure and impulse at 3.0 m from the tank centre (12.1 kPa) were generated during the $LH_2$ simulation.

Table 5. Results of the $LH_2$ BLEVE simulations: average overpressure and impulse of the blast wave along the three axes (transversal, longitudinal and vertical) at 3 m from the tank centre.

| Simulation | Pressure (Pa) | Temperature (K) | Overpressure (kPa) | Impulse (Pa·s) | Overpressure experiments (kPa) |
|---|---|---|---|---|---|
| LH2 | 1,101,325 | 32.10 | 12.1 | 42.4 | 14.3 |
| GH2 | | 32.93 | 11.3 | 13.9 | 14.3 |
| LH2-GH2 | | 32.10, 32.50 | 11.3 | 27.1 | 14.3 |

The results of the CFD parametric analysis were compared with the BMW bursting test series on $LH_2$ tanks [20] previously described are presented in Table 5. Only the maximum overpressure measured during the BMW tests for the initial tank pressure of 1,101,325 Pa is report in [20]. This comparison is not fully reliable because the effects of combustion and the cutting charges on the pressure were not simulated in the CFD analysis. Nevertheless, a good agreement between the experimental and numerical results was obtained by keeping in mind the previous considerations. Finally, it may be speculated that the difference in overpressure of 2.2 kPa corresponds to the combined effects of combustion and explosives.

### 4.1 Suggestions for development and improvement of analytical and empirical models

The ADREA-HF CFD code was validated in this study for $LCO_2$ BLEVE. The results of the CFD parametric analysis on $LH_2$ BLEVE may provide paramount indications on future modelling activities of hydrogen tank explosions as well as for different type of substances. The effect of the liquid and gaseous phases on the pressure wave behaviour might suggest modifications of existing analytical real gas behaviour models in which only one phase is considered. For instance, Birk et al. [34] developed a model to estimate the mechanical energy generated by the explosion based only on the vapour phase contribution, while only the liquid fraction was considered by the method proposed by Casal et al. [37]. Even though these models were validated for hydrocarbons BLEVE (e.g. propane and butane), they do not properly perform when the filling degree of the vessel is too low or too high [17,18]. As previously discussed, the amount of the flashing liquid during the expansion can be calculated by the CFD code and a correlation with the different initial conditions can be determined. For instance, the results obtained in this study might be compared with the formula provided by Prugh in [38] and suggest further modifications. Moreover, flashing of the liquid was recognised as responsible for the behaviour of the pressure wave in the near-field. Therefore, the CFD analysis could aid the near-field investigation, especially by supporting experimental works and have different implications in the development or improvement of analytical models. As result of this study, the ideal gas behaviour models seem to be an effective engineering tool to conduct a fast and reliable consequence analysis of BLEVE explosions. This conclusion is made by analysing the results obtained in [18] where the BMW tests were successfully simulated by means of ideal gas behaviour models.

## 5.0 CONCLUSIONS

This investigation analysed different aspects of the BLEVE phenomenon. The outcomes of the CFD analysis demonstrated the complexity of the BLEVE phenomenon. The ADREA-HF CFD code was validated by means of $LCO_2$ BLEVE experiments. A similar approach was employed to conduct a CFD parametric analysis of LH2 BLEVEs. The BMW bursting tank scenario tests on automotive $LH_2$ tanks were adopted as reference for this investigation. Good agreement with the experiments were achieved by the CFD parametric analysis. Several observations on the pressure wave dynamic generated by $LH_2$ BLEVE were highlighted in this study. The key points of these observations are the following:

- the differences in the behaviour of the pressure wave on the vertical and horizontal planes were highlighted.
- Both hydrogen phases contribute to the explosion yield i.e., similar maximum overpressure values were reached when the tank was filled with either $LH_2$ or $GH_2$.
- The GH2 simulation produces the shortest explosion and thus the smallest impulse value.
- Two pressure peaks are characteristic of the explosion of the 100% $GH_2$ simulations, while three peaks are generated for the 100% $LH_2$ cases.

- It is presumed that the maximum overpressure is not mainly affected by the hydrogen mass, while this parameter has an effect on the impulse of the blast wave.

The outcomes of the analysis conducted in this paper may suggest few modifications of existing analytical models employed for the BLEVE consequence analysis. Furthermore, some indications on future studies (both experimental and theoretical) to fulfil the dearth of knowledge on the BLEVE event, especially in the case of hydrogen technologies, were suggested heretofore. To summarised, the combustion should be modelled during the $LH_2$ BLEVE explosion simulation since hydrogen is a highly flammable gas. Both radiation and overpressure from the fireball should be evaluated. Moreover, the results of the CFD analysis may provide critical indications to the development of future analytical models for the BLEVE consequence analysis. Even the CFD codes can be further developed by implementing the nucleation and boiling models. Beyond the modelling activity, additional experiments must be conducted, especially in the case of cryogenic fluids. During the experiments, the focus can be placed on the consequences as well as on the probability of a failure in case of a double walled vessel. Thanks to the extreme high degree of insulation to limit the boil-off of the cryogenic $LH_2$, it is not certain that a BLEVE can occur even when the tank is exposed to a fire. This will be investigated during the $LH_2$ fire test of the Norwegian project “Safe Hydrogen Fuel Handling and Use for Efficient Implementation ($SH_2IFT$)”.

## ACKNOWLEDGMENTS

This work was undertaken as part of the research project “Safe Hydrogen fuel handling and Use for Efficient Implementation ($SH_2IFT$)”, and the authors would like to acknowledge the financial support of the Research Council of Norway under the ENERGIX programme (Grant No. 280964). Furthermore, the research leading to these results was financially supported by the PRESLHY project, which has received funding from the Fuel Cells and Hydrogen 2 Joint Undertaking under the European Union’s Horizon 2020 research and innovation program under grant agreement No 779613. This Joint Undertaking receives support from the European Union’s Horizon 2020 research and innovation programme, Hydrogen Europe and Hydrogen Europe research.

## REFERENCES

1. Ustolin, F., Paltrinieri, N. and Berto, F., Loss of integrity of hydrogen technologies: A critical review, *International Journal of Hydrogen Energy*, **45**, 2020, pp. 23809-23840.
2. McAllister, S., Chen, J.-Y. and Fernandez-Pello, A.C., Fundamentals of Combustion Processes, 2011, Springer Science +Business Media, LLC, New York.
3. NIST, NIST Chemistry WebBook, 2019, webbook.nist.gov/ (accessed 19.03.2019).
4. Barthelemy, H., Weber, M. and Barbier, F., Hydrogen storage: Recent improvements and industrial perspectives, *International Journal of Hydrogen Energy*, **42**, 2017, pp. 7254-7262.
5. DNV-GL, Energy Transition Outlook 2020 - A global and regional forecast to 2050, 2020.
6. FuelCellsWork, Norse Group Announces Launch of MF Hydra - World’s First LH2 Driven Ferry Boat, 2020, https://fuelcellsworks.com/news/norse-group-announces-launch-of-mf-hydra-worlds-first-lh2-driven-ferry-boat/ (accessed 16.03.2021).
7. Wilhelmsen, HySHIP project clinches EUR 8M funding award, 2020, https://www.wilhelmsen.com/media-news-and-events/press-releases/2020/hyship-project-clinches-eur-8m-funding-award/ (accessed 16.03.2021).
8. Newborough, M. and Cooley, G., Developments in the global hydrogen market: The spectrum of hydrogen colours, *Fuel Cells Bulletin*, 2020, pp. 16-22.
9. ten Kate, W., van den Noort, A., Vos M. and Özgün O., European Carbon Neutrality: The Importance of Gas, Report No.: OGNL.180049, 2020.
10. Delvosalle, C., Fievez, C., Pipart, A. and Debray, B., ARAMIS project: A comprehensive methodology for the identification of reference accident scenarios in process industries, *Journal of Hazardous Materials*, **130**, 2006, pp. 200-219.

11. Ustolin, F., Song, G. and Paltrinieri, N., The influence of H2 safety research on relevant risk assessment, *Chemical Engineering Transaction*, **74**, 2019, pp. 1393-1398.
12. Abbasi, T. and Abbasi, S.A., The boiling liquid expanding vapour explosion (BLEVE): Mechanism, consequence assessment, management, *Journal of Hazardous Materials*, **141**, 2007, pp. 489-519.
13. Eyssette, R., Heymes, F. and Birk, A.M., Ground loading from BLEVE through small scale experiments: Experiments and results, *Process Safety and Environmental Protection*, **148**, 2021, pp. 1098-1109.
14. Jovanović, A.S. and Baloš, D., INTeg-Risk project: Concept and first results, *Journal of Risk Research*, **16**, 2013, pp. 275-291.
15. Walls, W.L., What is a BLEVE?, *Fire Journal*, **31**, 1978, pp.46-47.
16. Abbasi, T. and Abbasi, S.A., The boiling liquid expanding vapour explosion (BLEVE) is fifty ... and lives on!, *Journal of Loss Prevention in the Process Industries*, **21**, 2008, pp.485-487.
17. Hemmatian, B., Planas, E. and Casal, J., Comparative analysis of BLEVE mechanical energy and overpressure modelling, *Process Safety and Environmental Protection*, **106**, 2017, pp. 138-149.
18. Ustolin, F., Paltrinieri, N. and Landucci, G., An innovative and comprehensive approach for the consequence analysis of liquid hydrogen vessel explosions, *Journal of Loss Prevention in the Process Industries*, **68**, 2020, 104323.
19. Casal, J., Hemmatian, B. and Planas, E., On BLEVE definition, the significance of superheat limit temperature (Tsl) and LNG BLEVE's, *Journal of Loss Prevention in the Process Industries*, **40**, 2016, 81.
20. Pehr, K., Aspects of safety and acceptance of LH2 tank systems in passenger cars, *International Journal of Hydrogen Energy*, **21**, 1996, 387-395.
21. Sintef, SH2IFT - Safe Hydrogen Fuel Handling and Use for Efficient Implementation, 2019, https://www.sintef.no/projectweb/sh2ift/ (accessed 02.09.2019).
22. PRESLHY, Prenormative Research for Safe Use of Liquid Hydrogen, Research and Innovation Action Supported by the FCH JU 2.0, 2019, https://preslhy.eu/ (accessed 22.06.2019).
23. van der Voort, M.M., van den Berg, A.C., Roekaerts, D.J., Xie, M. and de Bruijn, P.C., Blast from explosive evaporation of carbon dioxide: experiment, modeling and physics, *Shock Waves*, **22**, 2012, pp. 129-140.
24. Fürst, S., Dub, M., Gruber, M., Lechner, W. and Müller, C., Safety of hydrogen-fueled motor vehicles with IC engines, International Conference on Hydrogen Safety, Pisa, Italy, 2005.
25. Rybin, H., Krainz, G., Bartlok, G. and Kratzer, E., Safety Demands for Automotive Hydrogen Storage Systems, International Conference on Hydrogen Safety, Pisa, Italy, 2005.
26. Venetsanos, A.G., Papanikolaou, E. and Bartzis, J.G., The ADREA-HF CFD code for consequence assessment of hydrogen applications, *International Journal of Hydrogen Energy*, **35**, 2010, pp. 3908-3918.
27. Koutsourakis, N., Venetsanos, A.G. and Bartzis, J.G., LES modelling of hydrogen release and accumulation within a non-ventilated ambient pressure garage using the ADREA-HF CFD code, *International Journal of Hydrogen Energy*, **37**, 2012, pp. 17426-17435.
28. Giannissi, S.G., Venetsanos, A.G., Markatos, N. and Bartzis, J.G., Numerical simulation of LNG dispersion under two-phase release conditions, *Journal of Loss Prevention in the Process Industries*, **26**, 2013, pp. 245-254.
29. Giannissi, S.G., Venetsanos, A.G., Markatos, N. and Bartzis, J.G., CFD modeling of hydrogen dispersion under cryogenic release conditions, *International Journal of Hydrogen Energy*, **39**, 2014, pp. 15851-15863.
30. Giannissi, S.G., Venetsanos, A.G. and Hecht, E.S., Numerical predictions of cryogenic hydrogen vertical jets, *International Journal of Hydrogen Energy*, 2020, pp. 1–13.
31. Tolias, I.C., Venetsanos, A.G., Markatos, N. and Kiranoudis, C.T., CFD modeling of hydrogen deflagration in a tunnel, *International Journal of Hydrogen Energy*, **39**, 2014, pp. 20538–20546.

32. Tolias, I.C., Venetsanos, A.G., Markatos, N. and Kiranoudis, C.T., CFD evaluation against a large scale unconfined hydrogen deflagration, *International Journal of Hydrogen Energy*, **42**, 2017, pp. 7731-7739.
33. Tolias, I.C., Venetsanos, A.G., Kuznetsov, M. and Koutsoukos, S., Evaluation of an improved CFD model against nine vented deflagration experiments. *International Journal of Hydrogen Energy*, **46**, 2020, pp. 12407–12419.
34. Giannissi, S.G. and Venetsanos, A.G., Study of key parameters in modeling liquid hydrogen release and dispersion in open environment, *International Journal of Hydrogen Energy*, **43**, 2018, pp. 455–467.
35. Nasrifar, K., Comparative study of eleven equations of state in predicting the thermodynamic properties of hydrogen, *International Journal of Hydrogen Energy*, **35**, 2010, pp. 3802-3811.
36. Birk, A.M., Davison, C. and Cunningham, M., Blast overpressures from medium scale BLEVE tests, *Journal of Loss Prevention in the Process Industries*, **20**, 2007, pp. 194-206.
37. Baker, W.E., Cox, P.A., Kulesz, J.J., Strehlow, R.A. and Westine, P.S., Explosion Hazards and Evaluation, 1983, Elsevier Science, New York.
38. Casal, J. and Salla, J.M., Using liquid superheating energy for a quick estimation of overpressure in BLEVEs and similar explosions, *Journal of Hazardous Materials*, **137**, 2006, pp. 1321-7.
39. Prugh, R.W., Quantitative Evaluation of "BLEVE" hazards, *Journal of Fire Protection Engineering*, **3**, 1991, pp. 9-24.
40. Nayak, S., Garcia, S., Carreto, V. and Mannan, M.S., Can a liquid hydrogen storage tank BLEVE? AIChE Annual Meeting, 2011, p. 668–9.
41. Eyssette, R., Heymes, F., Crawford, J. and Birk, A.M., Near Field Effects of Small Scale Water BLEVE (Brebbia, C.A., Garzia, F. and Lombardi, M. Eds.), WIT Press, 2018, pp. 465-473.